Laves phase precipitation and its transformation kinetics in the ferritic stainless steel type AISI 441

By M.P Sello[1] and W.E Stumpf

Department of Materials Science and Metallurgical Engineering of the University of Pretoria, South Africa with [1] currently at BHP Billiton, Hillside Aluminium Smelter, 9 West Central Arterial, Richards Bay, 3900, South Africa.

Corresponding author: maitse_s@hotmail.com; cell: +27 72 514 3047, tel: +27 39 908 9433, fax: +27 86 219 4481

Abstract

Electrolytic extraction followed by XRD analysis of precipitates after isothermal annealing of an AISI 441 ferritic stainless steel between 600 – 850°C, produced the time–temperature–precipitation (*TTP*) diagram for the Fe_2Nb-Laves phase. The *TTP* diagram shows two classical C noses, the first one between 750 to 825 °C and the second one, estimated to be close to 650 – 675 °C. TEM analyses show two independent nucleation mechanisms, i.e. at about 600 °C nucleation takes place on dislocations but above 750 °C, grain boundary nucleation is dominant. The measured solvus temperature of 875 °C for Fe_2Nb in this steel is 50°C higher than predicted by Thermo–Calc®. Kinetic modelling at 800 °C agreed well with the experimental results for a surface energy of 0.435Jm^{-2} and an initial particle center-to-center separation distance on grain boundaries of about 0.2μm.

Keywords: Fe_2Nb, time-temperature-precipitation (*TTP*) diagram, Johnson-Mehl-Avrami-Kolmogorov (*JMAK*), *transformation kinetics*

1 Introduction

Ferritic stainless steel type AISI 441, a Ti and Nb dual stabilised ferritic stainless steel, is commonly used in the manufacture of catalytic converter shells in the automotive industry. The Cr, Nb and Ti alloying additions improve the stress-corrosion resistance and mechanical properties by solid solution hardening [1-3]. But these also lead to the formation of a variety of precipitates such as Nb(C,N) and Ti(C,N) (carbo–nitrides) and Fe_2Nb (Laves phase). The effect of these Nb precipitates on the high temperature strength of these steels appears to be still uncertain, but it has been reported that rapid coarsening of the Laves phase significantly reduced the high temperature strength [3,4] of the steel.

The effect of Laves phase in the embrittlement of this material was studied and has been reported elsewhere [5,6]. After solution treatment at 850°C the steel exhibited good room temperature impact toughness but above and below this solution temperature the impact toughness decreased sharply. Below 850°C the presence of the Laves phase played a significant role in the embrittlement of the steel whereas above that temperature, an increase in the grain size reduced the impact strength. These impact toughness results largely agree with phase equilibrium calculations by Thermo–Calc® whereby it was observed that a decrease in the Laves phase volume fraction with increasing solution temperature corresponds to an increase in the impact toughness of the steel. Annealing above 900°C where no Laves phase exists, grain growth is found which similarly has a very negative influence on the steel's room temperature impact properties. Where both a large grain size as well as Laves phase are present, it appeared that the larger grain size was the dominant embrittlement mechanism [6]. Annealing at 850°C where any grain size effect was minimal, the effect of cooling rate after heat treatment on Laves phase embrittlement was quantified with a significant decrease in the impact toughness with decreasing cooling rates down to 1°C s^{-1} that allowed Laves phase to form during slow cooling.

The objective of this work published here was to take the above study further by developing a kinetic model for the Laves phase precipitation process as a function of heat treatment and steel composition, as there is a general lack of thermodynamic and kinetic data of Laves phase formation and its effects in the manufacture of exhaust systems from type AISI 441 steel.

2 Experimental procedure

Table 1 shows the chemical composition of the three alloys that were used in this study, which were supplied by Columbus Stainless as 7.8 mm thick hot band materials, with Steel A that had been found to be brittle in the as received condition. Annealing was done in a tubular furnace with a type K thermocouple spot welded to the specimens while the start of the annealing time t_0 was considered from the point where the specimen had stabilised at the set temperature, generally after about 400 seconds. After annealing from 600 to 850°C for times of 5 to 1000 minutes, the specimens were quenched in water. The precipitates were then extracted electrolytically using 60% nitric acid in water at a potential of 5 V dc and the residue was vacuum suction filtered using a sub-micron glass filter paper (≤ 0.7 μm) while the filter paper had been pre-weighed to account for the very fine precipitates that may remain trapped in it during the filtration process. The extracted residues where finally rinsed with ethanol, dried and weighed to obtain the total weight fraction from the previously weighed steel specimen.

Table 1. Chemical composition (%wt) of the type 441 ferritic stainless steels.

Alloys	C	Cr	Mn	Mo	Si	Ti	Ni	N	Nb
Steel A	0.012	17.89	0.51	~0.00	0.50	0.153	0.190	0.0085	0.444
Steel B	0.023	17.90	0.35	<0.01	0.31	0.171	0.12	0.26	0.39
Steel C	0.014	18.30	0.45	1.942	0.47	0.106	0.15	0.016	0.251

XRD analyses of the precipitate residues were carried out on a PANalytical X'Pert Pro powder diffractometer with X'Celerator detector and variable divergence and receiving slits equipped with an Fe-filtered Co-K_α (λ = 1.789 Å) anode as a source of X-rays. Quantification of the various phases' weight fractions in the powder residue was carried using Autoquan/BGMN software (GE Inspection Technologies) employing a Rietveld refinement approach which enables the volume fraction–time relationship to be found with fair accuracy measured to within a standard deviation of 3σ error (that is a 99.7% confidence interval) [7].

The microstructures were characterized mainly by thinning discs for transmission electron microscopy (TEM), particularly to identify the precipitates by energy dispersive spectrometry (EDS). TEM observations were carried out between 160 and 200 kV. TThe TEM specimens were mechanically ground from both sides to less than 70 μm. Electropolishing was conducted until perforation of the disc using a twin jet electropolisher in 10% perchloric acid in 90% acetic acid solution at room temperature at a voltage of 55 dc.

3 Results

Fig. 1 shows the XRD analysis of the precipitate residue from the as received plant-brittle Steel A. Two main types of precipitates where detected, i.e., Laves phase and carbo-nitrides with some interference from the α-Fe matrix phase often also present. The results from this steel indicated that the weight percentages for the Laves phase and (Ti,Nb)(C,N) were about 1.14% and 0.33%, respectively. The lattice parameters of the Laves phase were also determined to be a_o= 0.481 nm and c_o = 0.784 nm, with c_o/a_o = 1.64, which is close to the $MgZn_2$ C14-type structure of the Laves phase. In the earlier work on these steels [5,6], this Steel A in the as received plant-brittle condition had a Charpy V-notch impact strength at room temperature of only 11 Joules, illustrating the severe embrittling effect of the 1.14% weight fraction Laves phase present in the microstructure.

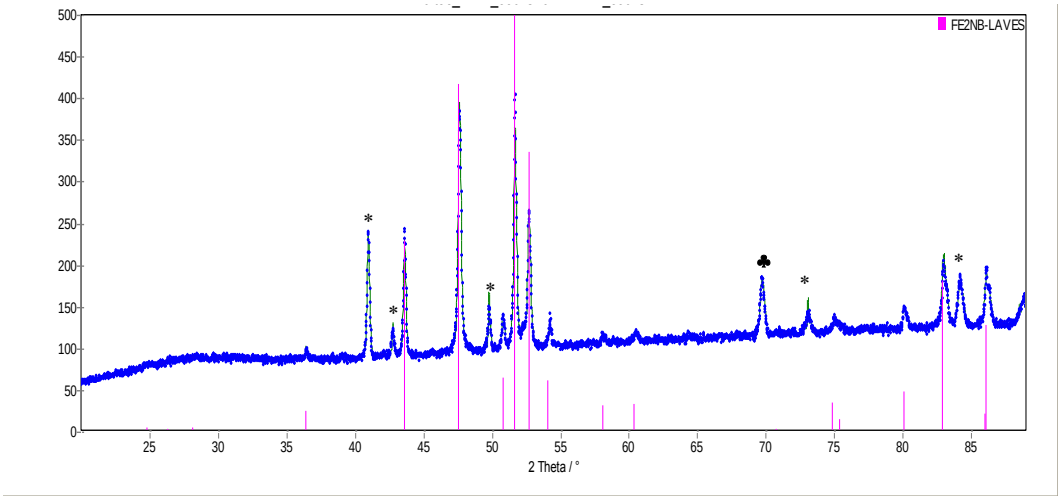

Fig. 1. A typical XRD scan of the electrolytically extracted precipitate residue from Steel A in the as received plant-brittle condition, showing the presence of the Laves phase peaks while the remaining peaks are the carbides and nitrides, indicated by (∗) and the α - Fe matrix, indicated by (♣).

3.1 Equilibrium Laves Phase Fraction in Steel A

Steel A was first annealed at 850°C (just above the solvus temperature of 825°C as predicted by Thermo-Calc® for Steel A) for 2 hours to dissolve the Laves phase while limiting excessive grain growth, and then water quenched. Specimens were thereafter annealed at various temperatures and for different times before quantifying the second phase contents. Fig. 2 shows the typical *S*-shaped curves for the Laves phase plotted from these analyses after converting the weight fractions to volume fractions using a molar volume of 2.36×10^{-23} m^3/mol for Fe_2Nb [5]. It was observed that for the specimens that were heated at 600°C, even after annealing for 1000 minutes, the Laves phase formation had not reached equilibrium and was still continuing. This indicates that although the chemical driving force for Laves phase nucleation should be relatively high at this temperature due to a high undercooling, the lowered diffusivity of Nb atoms at this temperature led to a low overall nucleation and growth rate. At 700°C it was also found that the formation rate of the Laves phase is much higher than at higher or lower temperatures, an observation that already hints at the possibility of a second lower temperature nose in a *TTP* diagram for this phase. A similar semi-quantitative observation was made by Sawatani et al [8] on a Ti and Nb stabilised low C, N – 19%Cr – 2%Mo stainless steel, where they observed that the Laves phase precipitates were in a far larger quantity after annealing at about 700°C than at other annealing temperatures. At 850°C in Fig. 2, the volume fraction of the Laves phase in Steel A reached a maximum of only 0.005%, and a proper *S*-curve could not be established. However, this already shows a discrepancy between the experimental evidence of a 0.005% volume fraction of Laves phase remaining at 850°C versus the Thermo-Calc® prediction that no Laves phase should be present at and above about 825°C in this composition of Steel A.

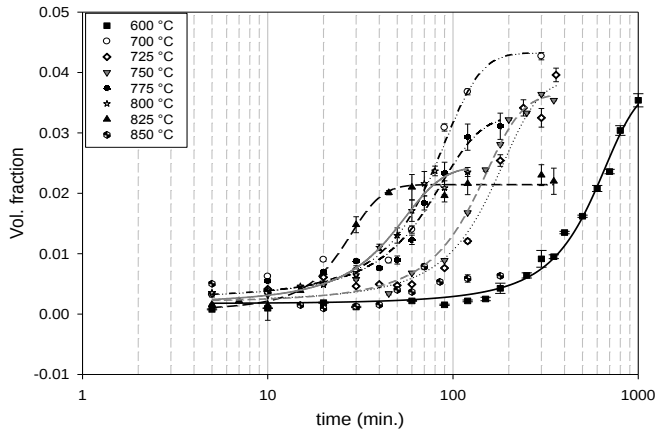

Fig. 2. The Laves phase volume fraction – temperature/time curves during isothermal annealing of Steel A in the temperature range 600 to 850°C.

3.2 Laves Phase Transformation Kinetics

The kinetics of an isothermal transformation is usually expressed by the modified Johnson–Mehl–Avrami–Kolmogorov (*JMAK*) type of equation:

$$V_v = 1 - \exp\left(-kt^n\right) \qquad [1]$$

where V_v is the Laves phase volume fraction, k is the reaction rate constant, and n is the time exponent. From Fig. 2, the measured points that fall between 5 and 95 percent on the *S*-curves (only on the specimens annealed in the temperature range of 700 – 825°C) were plotted in the {l*nln* [*1/*(*1-*V_v)]} vs {*ln t*} relationship, see Fig. 3. The time exponent values of n were found to generally range between 1.37 and 1.54. This suggests that Laves phase nucleation in this temperature range takes place on either plane or edge grain boundaries [9].

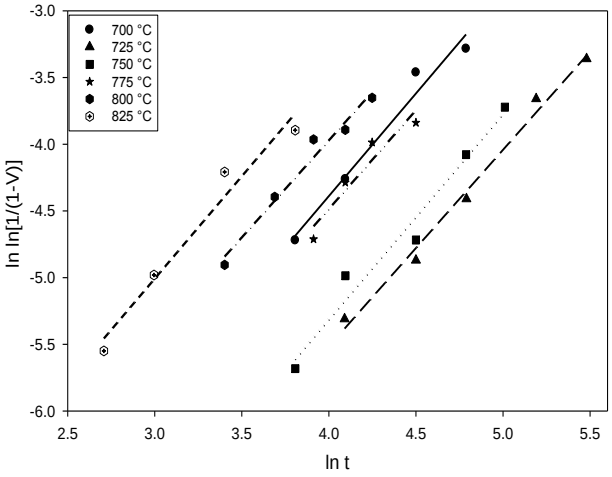

Fig. 3. The Laves phase transformation curves of Steel A between 700 and 825 °C according to the *JMAK* type of equation.

The activation energy Q for the Laves phase's formation was estimated from the reaction rate constant k and was found to be 211.3 kJ/mol, a value that is somewhat lower than the reported activation energy for

the volume diffusion of Nb in an Fe-Cr matrix of about 240 kJ/mol [10,11]. This measurement of the activation energy was carried out using only data from the temperature range of 750 to 825°C as it appears that the precipitation mechanism may be different at lower temperatures.

3.3 Temperature Effect on Isothermal Transformations

From Fig. 3 it was possible to complete an isothermal time-temperature-precipitation (*TTP*) transformation diagram for Steel A as shown in Fig. 4 for the measuring times ($t_{5\%}$ and $t_{95\%}$) for the beginning and end of transformation and for 50% transformation, i.e. $t_{50\%}$. From Fig. 4, it should be noted that the points from Fig. 2 at 600°C could not be used in the *TTP* diagram as equilibrium had not been reached and only estimated dashed lines for a second nose are shown below 700°C.

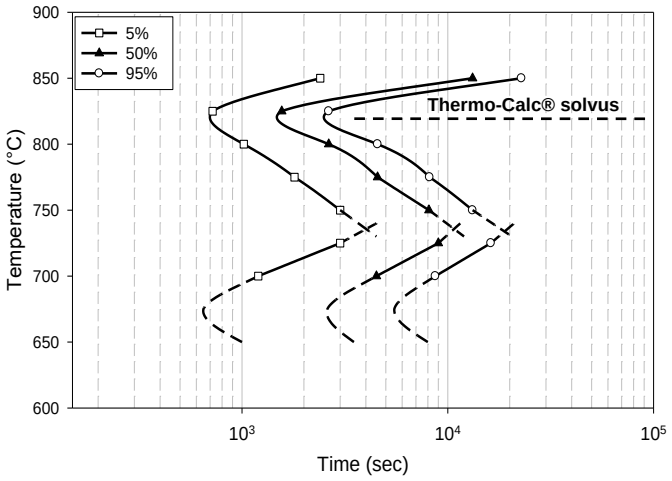

Fig. 4. A time – temperature – precipitation (TTP) diagram for the Laves phase formation in Steel A.

The results show the likely presence of two classical C noses on the transformation curves for Steel A, the first one occurring at a higher temperature of about 825°C and the second one at much lower temperatures, estimated to possibly be in the region of about 650 to 675°C. Because of extraordinarily long annealing times to reach equilibrium from the much slower diffusion, it was found to be impractical to find the exact point of this lower temperature nose. The available results, however, are sufficient to show that there are likely two different nucleation mechanisms within the Laves phase transformation. In the work done by Silva et al. [12] on the AISI 444 ferritic stainless steel (that is, similar to Steel C from this work) the authors have also estimated a nose of their transformation curve to be between 800 and 850°C. Thermo-Calc® predictions on this Steel A have predicted the solvus temperature of the Laves phase to be

825°C, but the experimental results indicate that the Laves phase still exists up to the temperature of 850°C with a solvus temperature rather close to 875°C, see Fig. 5.

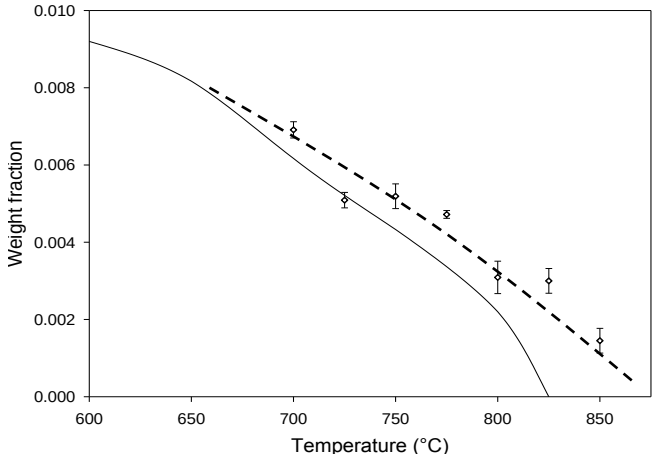

Fig. 5. Comparison between experimental and Thermo-Calc® calculated weight fractions of Laves phase in Steel A. The points and dotted line represent the experimental results while the full line is as predicted by Thermo-Calc® for this steel.

3.4 Effect of Grain Size on the Transformation Kinetics of Laves Phase in Steel A

Specimens from Steel A were first annealed at the respective temperatures of 850°C and 950°C for 2 hours and then water quenched. The corresponding linear intercept grain sizes were determined to be 49.9 µm and 152.1 µm, respectively from which the grain boundary surface areas per unit volume S_v were calculated to be 4.01×10^4 and 1.32×10^4 m^2/m^3 respectively, i.e. a difference of 67% in the potential nucleation site availability for grain boundary nucleation. Subsequently, the specimens were annealed at 750°C for different periods in order to compare the Laves phase transformation kinetics. Fig. 6 shows that the precipitation rate of the Laves phase is indeed retarded by the larger grain size, purely due to a smaller number of nucleation sites. However, an equal level of the maximum or equilibrium volume fraction could be achieved from both grain sizes, although at different annealing times, approximately an extra 400 minutes for the larger grain size. It is revealing to note that the difference in time to achieve the 50% transformation level in Fig. 6 is reasonably close to the earlier 67% difference in the grain boundary nucleation site availability. These results confirm that grain boundary nucleation of the Laves phase is of overriding significance in this steel at a temperature of 750°C. In a similar study done by Pardal et al. [13] on a superduplex stainless steel UNS S32750, the authors have made similar qualitative observations, but they did not determine the overall effect of the grain size on the volume fraction as was done here.

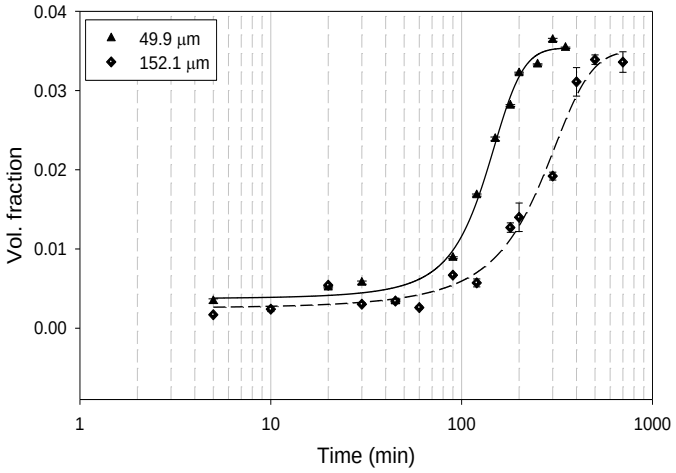

Fig. 6. Effect of grain size on the kinetics of the Laves phase transformation in Steel A at 750°C. The specimens were annealed first at 850 and 950□C respectively to set initial different grain sizes with minimal (at 850□C) or no (at 950□C) Laves phase present and were then annealed both at 750°C for different annealing periods.

3.5 Effect of the Steel's Composition on the Laves Phase's Transformation Kinetics

The effect of the steel's composition on the Laves phase kinetics was investigated comparing Steel A (0.444Nb–0.153Ti–~0Mo), with the Steel B (0.36Nb–0.171Ti–<0.01Mo) and Steel C (0.251Nb–0.106Ti–1.942Mo). The grain size of these materials was kept relatively constant and the transformation kinetics was investigated by annealing the specimens at 750°C over different periods of time. Fig. 7 shows the results which indicate that at 750°C, Steel A has a much higher volume fraction of Laves phase than Steels B and C, and this agrees with the Thermo-Calc® predictions for these three steels as shown in Table 2.

Fig. 7 also indicates that reducing the Nb and Ti contents as in Steel B (in comparison with Steel A), did not have any significant impact on the 50% volume fraction kinetics of the Laves phase precipitation but only on the final volume fraction. The addition of 1.94% Mo as in Steel C, however, has an impact by slightly retarding the 50% precipitation time of the Laves phase. Ahn et al. [14] have also observed that the precipitation of Fe_2Nb Laves phase in an 0.01C–0.38Nb–1.2Mo steel was slower than in an 0.01C-0.38Nb steel, and this was postulated to be due to Mo retarding the rate of Nb diffusion.

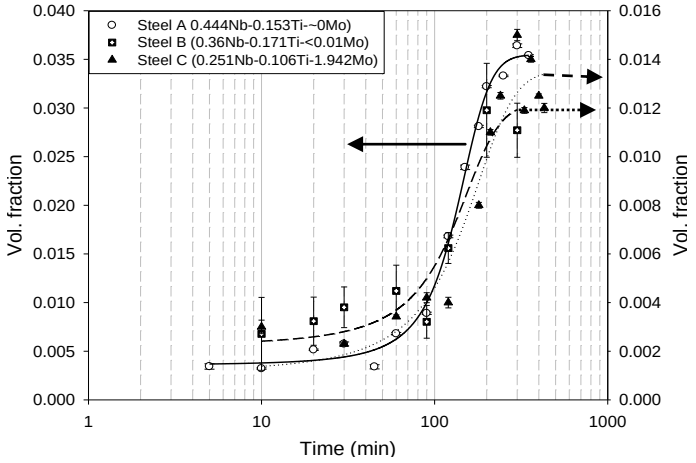

Fig. 7. Effect of the steel's composition on the Laves phase transformation kinetics. The specimens from these steels were all annealed at 750°C for different annealing periods (Maitse, I have shifted the positions of the arrows to make it more clear to which of the two axes they refer)

Table 2. Comparison between the Thermo-Calc® predictions and experimental values for the Laves phase weight fraction after annealing at 750°C to equilibrium conditions.

Temp. (°C)	*Weight fraction*	
	Thermo-Calc ®	*Experimental values*
Steel A	0.0041	0.0054
Steel B	0,0011	0,0013
Steel C	0.0029	0.0025

3.6 Microstructural Analysis of the Transformation Kinetics in Steel A

The nucleation mechanisms of the Laves phase during transformation were investigated in Steel A after annealing at 600, 750 and 800°C for 30 minutes, which allowed for a suitable time of precipitate growth, so that they could be analysed using TEM–EDX.

Fig. 8, shows the precipitate microstructure after annealing at 600°C. At the lower magnification (Fig. 8(a)) the remnant of the coarse grain boundary Laves phase precipitates could be found from the (later found to be inadequate!) solution treatment at 850°C for 2 hours. At a higher magnification (Fig. 8(b), the same area analysed from Fig. 8(a) is indicated by a circle, and the micrograph indicates that the nucleation sites for the Laves phase in this case are primarily on dislocations and subgrain boundaries. Remaining Laves phase precipitates in Fig.8(a) that present an asymmetrical shape on grain boundaries after the "solution treatment" at 850°C, may have a low mismatch with one grain but grow into the adjacent grain with which they do not have a rational orientation relationship because of that interface's higher surface energy and mobility. Similar observations were made by Li [15] in a 12Cr–2W steel with the nucleation and growth of the Fe_2W Laves phase.

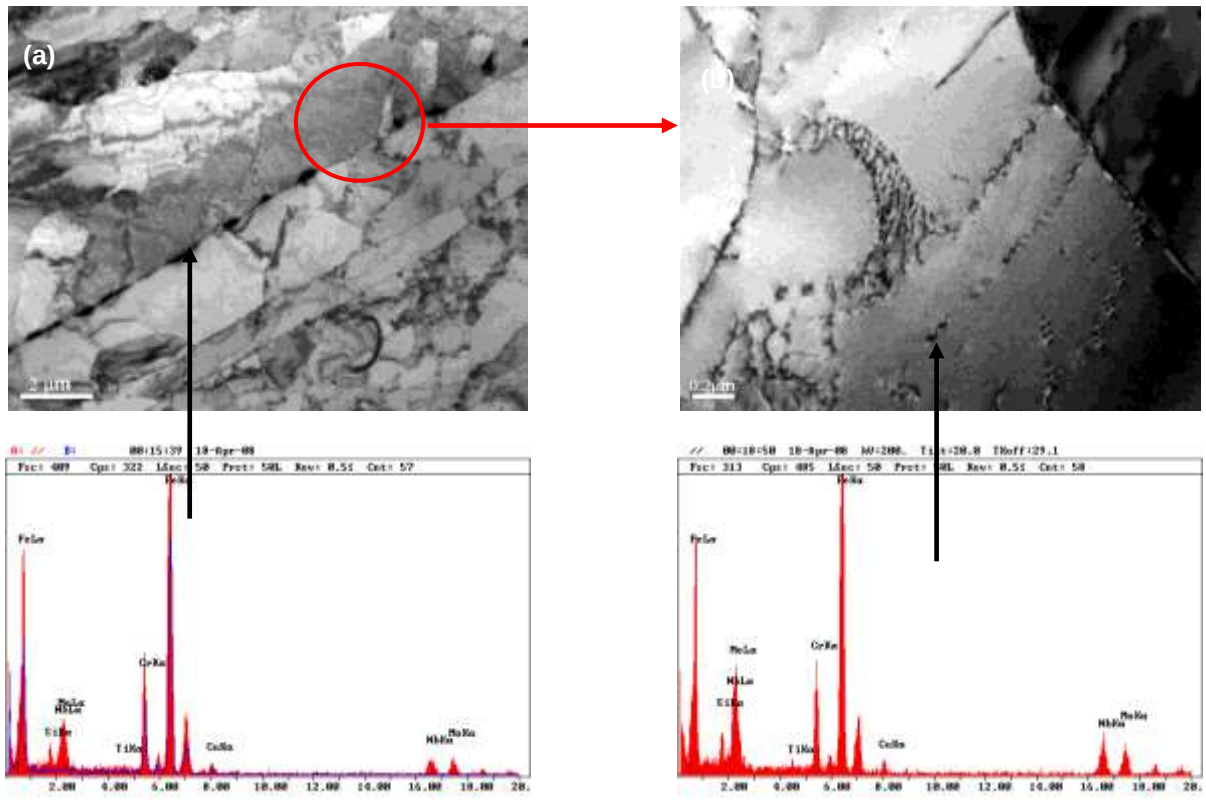

Fig. 8. TEM micrographs and Laves phase EDX spectra of the specimen of Steel A solution treated at 850°C for 2 hours then annealed at 600°C for 30 minutes; (a) a low magnification micrograph showing coarse grain boundary Laves phase precipitates possibly remaining from the inadequate solution treatment, and (b) the same area within the circle but at a high magnification, showing Laves phase precipitates nucleated at 600°C on subgrain boundaries and dislocations**.**

The microstructure of Steel A after annealing at 750°C is shown in Fig. 9. Comparing this specimen with the one that was annealed at 600°C in Fig. 8(b), the volume fraction of the Laves phase after only 30 minutes is already higher, suggesting a higher nucleation rate at 750°C. Also, there are more of the Laves phase grain boundary precipitates than dislocation precipitates, see Fig. 9(a). This suggests that the most preferred nucleation sites for the Laves phase at 750°C are the grain and subgrain boundaries, unlike as after annealing at 600°C, where primarily precipitation on dislocations occurred.

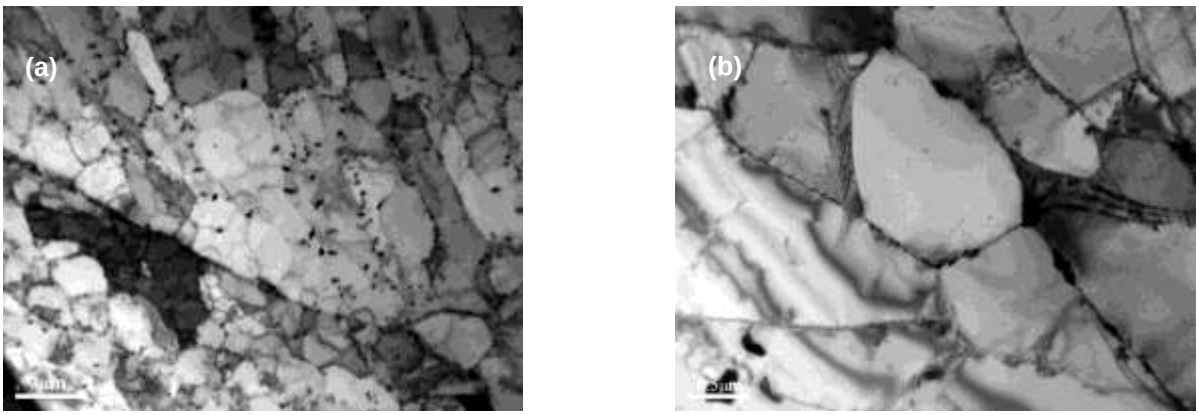

Fig. 9. TEM micrographs of Steel A solution treated at 850°C and then annealed at 750°C; (a) a low magnification micrograph showing grain and subgrain boundary Laves phase precipitates, and (b) at a higher magnification, showing Laves phase precipitates nucleated on the subgrain boundaries.

Fig. 10 shows the micrographs of the specimen after annealing at 800°C, which is heavily "decorated" with Laves phase precipitates on grain boundaries. At the higher magnification, it was observed that the preferred sites for the Laves phase nucleation are almost exclusively on grain boundaries, with very few precipitates on dislocations if compared to the specimen annealed at 600°C. Also, it can be observed that the presence of the dislocations in Fig 10(b) did not serve as preferred nucleation sites for the Laves phase as was the case at lower temperatures.

Comparing all three sets of microstructures, it is concluded that dislocations, subgrain and grain boundaries act as preferred nucleation sites for Laves phase precipitation. Analyses of the microstructures and also on the basis of the classical heterogeneous nucleation theory, demonstrate that nucleation on the grain boundaries is dominant at the higher annealing temperatures of 750°C and above, see Fig. 9 and Fig. 10, where the undercooling and hence the chemical driving force for nucleation are relatively low and the system then lowers its retarding force through grain boundary nucleation. As the temperature is decreased and the undercooling and hence the chemical driving force becomes higher, however, heterogeneous nucleation on dislocations becomes more significant.

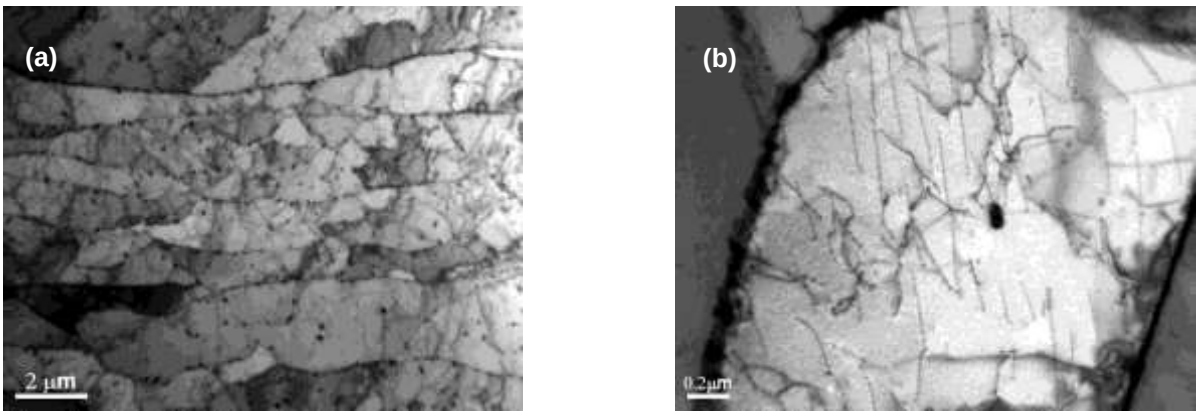

Fig. 10. TEM micrographs of the specimen solution treated at 850□C and then annealed at 800°C; (a) at a low magnification, showing grain boundary Laves phase precipitates, and (b) at a higher magnification showing Laves phase precipitates nucleated on the sub- and grain boundaries but not on dislocations.

4 Discussion

4.1 Nucleation

The nucleation rate under isothermal heterogeneous nucleation conditions and rate controlled by the slow diffusivity of Nb, can be presented by [9]:

$$\dot{N} = \bar{c} N_o \frac{kT}{h} \exp\left(-\frac{\Delta G^* + Q}{RT}\right) \qquad [2]$$

$$\Delta G^* = \frac{4\pi\gamma^3 \left\{2 - 3\cos\theta + \cos^3\theta\right\}}{3(\Delta G_v + \Delta G_\varepsilon)^2} \qquad [3]$$

where $\bar{c}$ is the Nb content in solution in the steel, N_o is the number of available nucleation sites per unit volume, k and h are the Boltzmann's and Planck's constants respectively, T is the absolute temperature, ΔG^* is the activation energy for nucleation, γ is the surface energy per unit area of the precipitate–matrix interface and θ is the contact angle between the Laves phase particle and the grain boundary. The critical embryo size r^* for forming a stable nucleus is then given by:

$$r^* = \frac{-4\gamma}{(\Delta G_v + \Delta G_\varepsilon)\left\{2 - \cos\theta - \cos^2\theta\right\}} \qquad [4]$$

where ΔG_v is the chemical free energy change per unit volume and ΔG_ε is the misfit strain energy around the particle, which is often relatively small compared to the chemical driving force ΔG_v and, hence, was neglected in the calculations of ΔG^* and r^*. The contact angle between the Laves phase and grain boundary was estimated from some TEM micrographs to typically lie between 20 and 30°.

4.2 Growth

To simplify this model, it is assumed that all the Laves phase precipitation occurs on grain boundaries and the growth and nucleation of the precipitates takes place simultaneously as it has often been observed that nucleation is superseded by growth very early within the precipitation process [16-18]. The growth of the precipitates is assumed to be controlled by the diffusion of Nb in the ferrite matrix. Assuming that the particle size is large enough, the position of the interface under one dimensional parabolic growth, which corresponds to the radius r of large spherical particles, is given by [3,19-21]:

$$r = \Omega\sqrt{D_{Nb}t} \quad \text{with} \quad \Omega \approx \sqrt{2\frac{\bar{c} - c^{\alpha\beta}}{c^{\beta\alpha} - \bar{c}}} \qquad [5]$$

where D_{Nb} is the Nb diffusion coefficient in ferrite, t is the reaction time, Ω is the supersaturation, $\bar{c}$ is the Nb content of the alloy $c^{\alpha\beta}$ and $c^{\beta\alpha}$ are the equilibrium concentrations in the ferrite matrix α and in the precipitate β (i.e. the Laves phase, Fe_2Nb), respectively. If $c^{\alpha\beta}$ is approximated by the solute concentration in the matrix after ageing for a long period of time and which is obtained from Thermo–Calc®, the supersaturation Ω of Nb for each steel can be calculated as shown in Table 3.

Table 3. Calculated equilibrium mole fractions at the interface Fe_2Nb / ferrite for Nb between 600 and 800 °C in AISI type 441 ferritic stainless steel.

Temperature (°C)	$X_{Nb}^{\alpha\beta}$ for Fe_2Nb (mole fraction)	$X_{Nb}^{\beta\alpha}$ in ferrite (mole fraction)	Supersaturation, Ω
600	2.25×10^{-3}	5.80×10^{-4}	1.410
650	2.00×10^{-3}	8.30×10^{-4}	1.411
700	1.50×10^{-3}	1.33×10^{-3}	1.414
750	1.00×10^{-3}	1.83×10^{-3}	1.416
800	4.20×10^{-4}	2.41×10^{-3}	1.420

The supersaturation of Nb for Steel A annealed between 800°C and 600°C, does not vary significantly and therefore the growth of the particles appears to be controlled by the diffusion rate. It is further assumed that the nucleation rate $\dot{N}$ for the Laves phase that led up to the growth stage is a constant and that soft – impingement does not occur. At time t the radius of the particle nucleated at time t_1 ($0 < t_1 < t$) is expressed by Equation 5. Assuming a spherical particle, the growth rate G_r at time t_1 is given by:

$$G_r = 4\pi r^2 \frac{dr}{d(t - t_1)} \qquad [6]$$

Therefore, the number of nuclei precipitated between t_1 and $t_1 + dt_1$ is $\dot{N}\, dt_1$. The rate of increase in the volume of all the particles formed at t_1 is then given by:

$$\frac{dV}{dt} = \frac{8\sqrt{2}}{3}\pi D_{Nb}^{3/2}\left[\frac{\bar{c} - c^{\alpha\beta}}{c^{\beta\alpha} - \bar{c}}\right]^{\frac{3}{2}} \dot{N}(t - t_1)^{\frac{3}{2}} \quad [7]$$

To convert Equation 7 into the volume fraction of the precipitates V_v, this equation is multiplied by $(\bar{c} - c^{\alpha\beta})/(c^{\beta\alpha} - \bar{c})$. By considering this composition factor and integrating Equation 7, the following equation for the volume fraction can be obtained [13,14]:

$$V_v = 1 - \exp\left\{-\frac{16\sqrt{2}}{15}\pi D_{Nb}^{3/2}\left[\frac{\bar{c} - c^{\alpha\beta}}{c^{\alpha\beta} - \bar{c}}\right]^{\frac{1}{2}} \dot{N}t^{\frac{5}{2}}\right\} \quad [8]$$

Equation 8 above, is the typical Johnson-Mehl-Avrami-Kolmogorov (*JMAK*) type of equation to describe the kinetics of the precipitating Laves phase in an AISI type 441 steel and utilising Thermo–Calc® software to predict the driving forces.

4.3 Parameters Required for Calculations

The chemical free energy change per unit volume ΔG_v of precipitate is given by:

$$\Delta G_v = \frac{\Delta G}{\upsilon V_v} \quad [9]$$

where V_v is the equilibrium volume fraction and υ the molar volume of the Laves phase, and ΔG is the molar free energy change of the precipitation reaction and is obtained from the Thermo-Calc® software, which leads to the solubility product for the Laves phase Fe_2Nb in Steel A with weight percentage of:

$$\log [Nb] = -2968.6/T + 0.1569 \quad [10]$$

This expression differs from the one obtained by Fujita and co-workers [22] in their recent work on niobium alloyed ferritic stainless steels, also for the Laves phase:

$$\log [Nb] = -3780.3/T + 2.4646 \quad [11]$$

4.4 Activation energies and critical radii

The following assumptions for the Laves phase transformation kinetics were used; (i) no treatment of soft impingement was introduced during the nucleation and growth stage, (ii) the normalised particle–size distribution at different nucleation times and growth rates remained constant and (iii) that the precipitation proceeds in an Fe–Nb–C alloy system and takes place only on grain boundaries, i.e. any precipitation on subgrain boundaries was excluded from the model. Also, from the results of both the XRD and Thermo-Calc® calculations, as the volume fraction of the carbo-nitride had shown no significant change, only the nucleation and growth of Laves phase was assumed to be taking place. Finally, the density of nucleation sites N_0 was estimated to be about 1×10^{18} m^{-3} from the measured grain size and hence the grain boundary

area per unit volume S_v of 4.10x10^4 m^2.m^{-3} and the observed center-to-center Laves phase separation distance of about 0.2 μm as shown typically in Fig. 10(b). There is one unknown parameter, the interfacial energy γ and this is treated as a fitting parameter. The calculations were carried out at 800°C and the parameters that were used for the Laves phase formation are shown in Table 5. The diffusion coefficient for niobium in ferrite is given by [10]:

$$D = D_o 1.5x10^{-4} \exp\left(\frac{-240000}{RT}\right) \quad [10]$$

where R = 8.314 J mol^{-1} K^{-1} is the universal gas constant and T is the absolute temperature. As 800°C is substantially above 0.5T_m in absolute temperatures, volume diffusion is assumed to be more prominent in this model than grain boundary diffusion.

Table 5. Parameters used in the calculations for Laves phase formation on grain boundaries.

Parameters	Values
Unit cell volume, V_{cell} (m^3)	1.57 x 10^{-28}
Molar volume, υ_m for Fe_2Nb (m^3/mol)	2.36 x 10^{-23}
Density, ρ of Fe_2Nb (kg/cm^3)	8.58
Lattice parameter, of bcc α–Fe (nm)	0.28
Contact angle, θ (°)	24

The activation energy for nucleation ΔG^* and the critical particle size r^* for the Laves phase's nucleation were calculated from Equations 3 and 4, assuming the surface energy of the Laves phase γ to be 0.435Jm^{-2} are shown in Table 6 below.

Table 6. The calculated values of the free energy change ΔG, the driving force ΔG_v, the activation energy for the nucleation ΔG^*, and the critical particle size r^* for the Laves phase's nucleation at 800°C.

Temp. (°C)	ΔG (J/mol)	ΔG_v (J/mol)	ΔG^* (J)	r^* (nm)
800	-90	-2.30x10^8	1.20x10^{-19}	32.5

4.4.1 Volume Fractions

Calculated volume fractions from Equation 8 for the Laves phase during isothermal annealing at 800°C are shown in Fig. 11 using γ = 0.435 Jm^{-2} as a fitting parameter and is compared to the corresponding experimental S-curve. Note that Equation 8 does not lead to an actual estimate of the absolute volume fraction within the steel at any point but predicts only the accumulated volume fraction of the Laves phase during the transformation kinetics. Therefore, for comparison purposes the experimental values had to be normalised with respect to their equilibrium volume fraction in this figure.

Inherent in Equation 8 is the fact that a large particle, which has nucleated within the early stages of precipitation, grows continuously even while the volume fraction approaches equilibrium. Because of the

capillary effect, small particles which nucleated late begin to dissolve from coarsening even though the large ones continue to coarsen. It has been demonstrated that the mean particle radius at first increases approximately parabolically with time as all the particles initially grow from supersaturated solid solution [23].

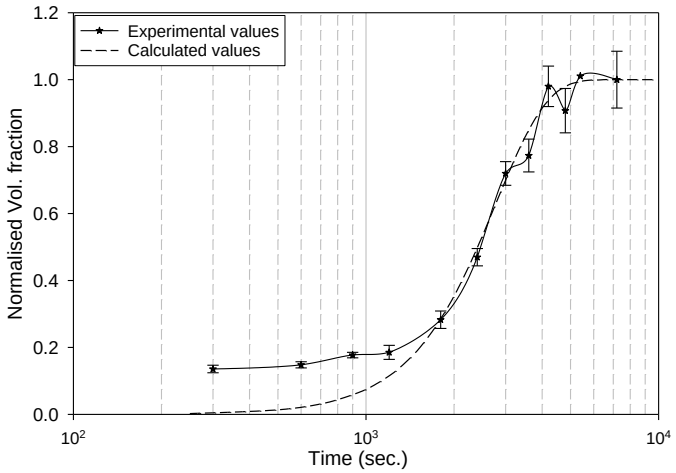

Fig. 11. Comparison between the experimental data and calculated isothermal transformation curves for the Laves phase's precipitation at 800 °C in the AISI type 441 ferritic stainless steel, with N_o = 1 x 10^{18} m^{-3} and γ = 0.435Jm^{-2}. Note that the experimental data does not reach a normalized volume fraction of zero as the initial solution treatments were all based on the (erroneous) Thermo-Calc® solvus value of 850°C instead of the later determined 875°C.

Although the predicted curve fits quite well with the experimental one, the question of course arises of how valid are the fitting parameter 0.435 J/m^2 for the surface energy as well as the estimated value of 1x10^{18} m^{-3} for the initial nucleation site density? Firstly, a value for the surface energy of 0.435 J/m^2 is reasonable as the Laves phase is known to be incoherent, hence its preference for heterogeneous nucleation on grain and subgrain boundaries as well as a reported rapid coarsening rate at high temperatures [3,4]. Secondly, an estimate of the value of 1x10^{18} m^{-3} for the initial nucleation site density was based on the measured grain boundary area only and ignored any nucleation subgrain boundaries. Should it have been possible to add this area of potential nucleation sites also to the estimate, the center-to-center separation distance of Laves particles would have to be larger than the observed 0.2 μm from Fig. 10(b), possibly something more as seen in Fig 10(a). The sensitivity of the number density of the nucleation sites N_o and the interfacial energy γ on the S-shaped transformation curve has been established in the niobium–alloyed ferritic stainless steel also for M_6C carbides by Fujita et al [19] and it was observed that their results are affected more by the interfacial energy than by the number density. This is to be expected because of the γ^3 term appearing in the activation energy ΔG^* in the exponential part of the nucleation equation.

When the experimentally determined activation energy (that is, Q = 211 kJ/mol within the temperature range of 750 to 825°C) for the Laves phase transformation kinetics is employed in the model, this gives

the initial nucleation site density N_o as approximately 2.2×10^{14} m^{-3} at 800°C, i.e. about 4.5 thousand times lower, a value that would lead to a particle separation distance on grain boundaries as high as about 9 μm, which does not agree with the typical observations at 800°C in Fig 10.

4.5 Summary

This modeled JMAK equation agrees reasonably well with the experimental data and analyses of the microstructures and also agrees qualitatively with the basis of the classical heterogeneous nucleation theory. For instance, it demonstrates that nucleation of the Laves phase on grain boundaries (where the initial nucleation site density N_o is relatively much lower than for homogeneous nucleation), is dominant at the higher annealing temperatures of 800°C and above, where the undercooling ΔT and hence the driving forces ΔG_v for nucleation are relatively low and the system then lowers its retarding forces through grain boundary nucleation. As the temperature is decreased and the undercooling ΔT and hence the driving forces are higher, however, heterogeneous nucleation on dislocations becomes more significant, and hence, the initial number of the nucleation sites N_o becomes higher. This parameter has a significant impact on the transformation kinetics of the Laves phase, and any increase in the number results in a decrease in the formation rate.

5 Conclusions

- A time–temperature–precipitation (*TTP*) diagram for the Laves phase in stainless steel AISI 441 that was determined from the transformation kinetic curves, appears to show two classical noses, i.e. the first one occurring at higher temperatures of about 750 to 825°C and the second one at much lower temperatures, estimated to possibly be in the range of about 650 to 675°C. Transmission electron microscopy (TEM) analyses show that there are two independent nucleation mechanisms at these respective temperature ranges. At lower temperatures of about 600°C, nucleation takes place principally on dislocations and as the annealing temperature is increased to above 750°C, grain boundary nucleation becomes more dominant.
- The effects of grain size and Mo additions on the transformation kinetics of the Laves phase, show that, by increasing the grain size or adding the alloying element Mo to AISI 441 stainless steel, that the rate of formation as well as the equilibrium quantity of the Laves phase formed, is lowered.

- For the kinetics at 800°C and by assuming an interfacial energy of 0.435Jm^{-2} for the incoherent Laves phase and estimating the nucleation site density on grain boundaries N_0 as 1x10^{18}m^{-3} from the measured grain size of 49.9μm which gives an observed 0.2μm particle center-to-center separation distance, the modelled S-shaped transformation curve agrees well with the experimental one at 800°C.

Acknowledgements

The authors would like to acknowledge the support of this work from Columbus Stainless, South Africa and the Department of Materials Science and Metallurgical Engineering of the University of Pretoria. The authors also kindly acknowledge permission to publish from both Columbus Stainless and the University of Pretoria.

Reference

1. N. Fujita, K. Ohmura, M. Kikuchi, Scripta Mater. 35 (1996) 705.
2. G. M. Sim, J. C. Ahn, S. C. Hong, Mater. Sci. Eng. A 396 (2005) 159.
3. N. Fujita, H. K. *D.* H. Bhadeshia, M. Kikuchi, Model. Simul. Mater. Sci. Eng. 12 (2004) 273.
4. D.G. Morris, M. A. Muñoz-Morris, C. Baudin, Acta Mater. 52 (2004) 2827.
5. M. P. Sello, PhD Thesis, University of Pretoria, June 2009.
6. M. P. Sello, W.E Stumpf, Mater. Sci. Eng. A 527 (2010) 5194.
7. L.B McCuster, R.B. Von Dreele, D. E. Cox, J. Appl. Crystallogr. 32 (1999) 36.
8. T. Sawatani, S. Minomina, H. Morikawa, Trans. ISIJ 22 (1982) 173.
9. J. W. Christian, The theory of transformations in metals and alloys: Part 1 second ed. Pergamon Press, Oxford, 1975..
10. J. Fridberg, L. Torndal & M. Hillert, Jern-kontorets Ann. 153 (1969) 263.
11. N. Fujita, H. K. D. H. Bhadeshia & M. Kikuchi, Metall. Mater. Trans. A 33A (2002) 3339.
12. C. C. Silva, J. P. Farias,H. C. Miranda, Mater. Charact 59 (2008) 528.
13. J. M. Pardal, S. S. M. Tavares, M. Cindra Fonseca & J. A. de Souza, Mater. Charact. 60 (2009) 165.
14. J. C. Ahn, G. M. Sim, K. S. Lee, Mater. Sci. Forum, 475 – 479 (2005) 191.
15. Q. Li, Metall. Mater. Trans A 37A (2006) 89.
16. A. Kosta, K. G. Tak, R. J. Hellmig, Acta Mater. 55 (2007) 539.
17. D. Rasmakrishma, S. P. Gupta, Scripta Metall. 20 (1986) 355.

18. D. Rasmakrishma, S. P. Gupta, Mater. Sci. Eng. 92 (1987) 179.
19. N. Fujita, K. Ohmura, A. Yamamoto, Mater. Sci. Eng. A 351 (2003) 272.
20. H. Yu, Y. Kang, Z. Zhao & H. Sun, J. Iron Steel Research, Int. 13 (2006) 30.
21. Y. Kang, H. Yu, J. Fu, K. Wang & Z. Wan, Mater. Sci. Eng A351 (2003) 265.
22. N. Fujita, K. Ohmura & M. Kikuchi, ISIJ Int. vol. 43, No. 12, (2003) 1999.
23. H. K. D. H. Bhadeshia, Mater. Sci. Forum 426 – 432 (2003) 35.